Applied Magnetic Resonance (2021) 52:1451–1479
https://doi.org/10.1007/s00723-021-01383-6

Applied
Magnetic Resonance

REVIEW

Oxygenation Status of Malignant Tumors vs. Normal Tissues: Critical Evaluation and Updated Data Source Based on Direct Measurements with pO_2 Microsensors

Peter Vaupel[1,2,3] · **Ann Barry Flood**[4] · **Harold M. Swartz**[4,5,6]

Received: 5 March 2021 / Revised: 20 June 2021 / Accepted: 30 June 2021 /
Published online: 19 July 2021

Abstract

Immature and chaotic vascular networks with critically increased intervascular distances are characteristic features of malignant tumors. Spatial and temporal heterogeneities of blood flow and associated availabilities of O_2, together with limited diffusive O_2 transport, and -in some patients- anemia, obligatorily lead to tumor hypoxia (=critically reduced O_2 levels) on macro- and microscopic scales. This detrimental condition, recently classified as a key hallmark of malignant growth, acts (a) as a barrier in most antitumor treatments, and (b) leads to malignant progression based on hypoxia-induced changes of the genome, transcriptome, and proteome, and finally to poor patient survival. This knowledge is, to a great extent, based on the systematic detection of tumor hypoxia in the clinical setting since the late 1980s. Precise assessment of the tumor oxygenation status was made possible using minimally invasive polarographic pO_2 microsensors in a series of research projects. To assess tumor hypoxia in the clinical setting, it is highly desirable to use technologies with (a) high spatial and temporal resolutions, (b) the capability to judge the severity of tumor hypoxia, (c) to allow mapping of pO_2 of the whole tumor mass, and (d) to enable serial investigations in order to verify treatment-related changes in tumor hypoxia. Selection and treatment of cancer patients according to their individual tumor oxygenation/hypoxia status for intensified and/or personalized hypoxia-targeted treatment strategies should be the ultimate goal.

1 Introduction

Hypoxia characterizes a deficient oxygenation status and is distributed heterogeneously within and across tumors. Spatial and temporal heterogeneities of tissue hypoxia on a micro- and macro-scopic scale as well as pronounced differences in the severity of hypoxia (hypoxia levels) are a principal hallmark of most cancer types

✉ Peter Vaupel
vaupel@uni-mainz.de

Extended author information available on the last page of the article

because they directly affect or even cause many other hallmarks. Since the early 1990s hypoxia has been recognized as a detrimental condition, which in turn critically influences a variety of biologic responses that increase the malignant potential through changes in the genome, transcriptome, and proteome [1]. In addition, hypoxia can act as a barrier to the effectiveness of most treatment modalities. Tumor hypoxia is also often observed to co-localize with other cellular "stresses" like lactate accumulation (up to 40 mM), adenosine accumulation (up to 100 μM), extracellular acidosis (pH < 6.8) and/or glucose deprivation (< 1 mM) [2]. Taken together, tumor hypoxia is associated with a poor prognosis.

1.1 Defining Levels of Hypoxia

This paper uses a rather rudimentary summary of critical oxygen partial pressure/pO_2 levels ("pO_2 cutoffs") for hypoxia divisions encompassing mild, moderate, and extreme (= severe) hypoxia, because the different thresholds are not well defined nor agreed upon. Furthermore, there is no clear declaration of hypoxia exposure times in order for a tissue to be described as 'having mild hypoxia' and so forth.

Nevertheless, the definitions used below, followed by a brief description of the potential pro-tumor consequences of having regions with critically low oxygen in tumors, give a rough picture of the current situation with which the clinician is confronted during tumor detection and therapy.

Tissue anoxia is the pathophysiological condition defined by the absence of oxygen, i.e., $pO_2 = 0$ mmHg[1] ("complete lack of oxygen"). Because some pathophysiological processes can adapt to functioning in anoxic conditions, some of the same genomic changes described below for extreme hypoxia can occur even in the absence of oxygen, i.e., tissue anoxia does not necessarily lead to cell death or regions of tumor necrosis.

Extreme hypoxia ($pO_2 < 1$ mmHg). Genomic changes, i.e., genomic instability, mutations, and genomic heterogeneity usually occur in situations with *extreme/severe hypoxia*. Increased genomic instability and mutation rates are especially pronounced in extreme hypoxia followed by reoxygenation. The selection and expansion of cell clones with permanent genomic changes favoring cell survival can in turn promote malignant progression, which is decisive for prognosis [1, 2].

Moderate hypoxia ($pO_2 < 10$ mmHg) can lead to reversible, adaptive alterations (i.e., stimulation or inhibition) of gene expression as well as posttranscriptional and post-translational modulations that result in changes in the cancer cell proteome. It is these changes that in turn facilitate multiple pro-tumor effects, including apoptosis resistance, unrestricted proliferation, epithelial-mesenchymal transition (EMT), migration, local invasion, and metastatic spread, poorly organized and chaotic tumor

[1] For readers more familiar with kilopascals, 1 mmHg = 0.133 kPa, 1 kPa = 7.519 mmHg.

angiogenesis, metabolic reprogramming, development of the Warburg phenotype, and recruitment of pro-tumor immune cells and inhibition of antitumor immune responses [3–6].

Mild hypoxia ($pO_2 < 20$ mmHg). Oxygen partial pressures characterizing *mild hypoxia* can also result in several progressive effects that are pro-tumor. These include (a) a progressive decrease in the radiosensitivity of cancer cells on exposure to X- and γ- radiation, (b) potentially compromising some chemotherapy (e.g., bleomycin, doxorubicin, platinum compounds), (c) possibly acting as an adverse parameter in antihormonal therapy, (d) potentially inducing resistance to hormonal treatment, and (e) becoming an obstacle to using photodynamic therapy (e.g., [7]). Finally, mild hypoxia may also lead to the release of reactive oxygen species (ROS) and HIF- activation.

In this rather rudimentary summary of critical pO_2 levels ("pO_2 cutoffs") for hypoxia divisions encompassing mild, moderate, and severe hypoxia, the different thresholds are not well defined. In addition, there is no clear declaration of hypoxia exposure times. Nevertheless, they give a rough picture of the situation with which the clinician is confronted during tumor detection and therapy. Assessment of the size of hypoxic sub-volumes and different severity of hypoxia in tumors, therefore, should be a "sine qua non" condition before and during treatment to guarantee effective personalized (individualized) therapy [8].

1.2 Clinical Implications

Based on the (a) hypoxia-induced malignant progression and (b) the hypoxia-related barriers to therapy as described above, hypoxia has been considered to be a powerful, independent, and adverse prognostic (or predictive) factor in clinical oncology since the early 1990s [9]. Thus, as a part of deciding on the best course of treatment, monitoring for interim outcomes and changes in oxygen, and assessing and refining prognosis, subtle assessments of tumor hypoxia (e.g., its severity and extent of macro- and micro-regional heterogeneities) should be a mandatory component of patient care both before and during treatment.

Nonetheless, there are significant barriers to operationalizing such assessments that have prevented its universal application in clinical settings. To overcome the current impediments to using measures of hypoxia in cancer treatment, it is important both to design hypoxia-detecting tools that are capable of providing high resolution in a clinically acceptable way and to design individualized treatment strategies considering heterogeneities and severity (= level, extent) of hypoxia that can result in clinically significant improved care [8].

Below, we expand on the complexities of understanding the importance of levels of oxygen in tumors. Table 1 illustrates this complexity by listing the major parameters that affect both the supply of oxygen to tissues as well as the factors that influence the demands for consuming oxygen. As detailed in Table 1, directly assessed oxygen partial pressures in tumors, which constitute the driving force for diffusive transport, are the result of a plethora of different determinants. We turn next to

Table 1 Major parameters determining the oxygenation status of tumors (selection)

A. Determinants of the oxygen supply (availability)
Perfusion (microregional limitations, flow rate, flow distribution, perfusion shunts, interstitial fluid pressure, fluctuating ischemia)
Diffusion (microregional limitations, microvascular geometry, size of interstitial space, water content, diffusion shunts)
O_2-capacity of the blood (overall and microregional reductions)
B. Determinants of the oxygen demand
Cell density (cellularity), tumor type (cell line)
Proliferation rate/growth rate, number of proliferating cells
Size of the stromal compartment, composition of the interstitial space,
Water content (~ 10% higher than in normal tissues)
Fraction of necrotic/apoptotic cells
Impact of hostile tumor microenvironment (TME)
Availability of nutrients (e.g., glucose, glutamine)
Role of metabolic reprogramming, expression of the Warburg effect
Role of the reverse Warburg effect
Maintenance of ATP/energy homeostasis
Maintenance of redox homeostasis
Maintenance of trans-membranous gradients (pH, ions)
Tissue temperature (HbO_2-binding, O_2-consumption rate, O_2- diffusivity)
Primary vs. metastatic lesions
Tumor growth in pre-irradiated regions (tumor bed effect)
Impact of antitumor immune responses
Protumor inflammatory processes
Trans-membranous transport of substrates and metabolites

measures of levels of oxygen that attempt to capture both the availability and the consumption of oxygen in tissues and how that influences diffusion.

2 O_2 Extraction: A Principal Parameter Determining the Spatial and Temporal Oxygen Distribution in Tumors

O_2 extraction rate (= O_2 consumption/O_2 availability-ratio) is the key measure of the adequacy of the O_2 supply to an organ or tissue. O_2 extraction is a comprehensive parameter which is greatly determined by parameters describing the "quality" of blood flow through tissues.

A strong inverse correlation was found between the extraction rate and median pO_2 values, both for malignant tumors and normal tissues [10]. At comparable O_2 extraction values, the median pO_2 in solid tumors was substantially lower than those in normal tissues. This finding clearly mirrors the pronounced limitations in the convective and diffusive O_2 delivery.

3 Critical Oxygen Diffusion Distances in Tumors: A Numbers Game

In 1955 Thomlinson and Gray [11] published a frequently quoted paper, describing tumor cords from a human bronchial carcinoma with central necrosis separated by a band of viable tumor cells 100–150 μm wide. However, in this study (and others) data were used to calculate O_2 diffusion distances that were completely unrelated to the tumor type of interest.

For these earlier calculations to be correct, diffusion-parameters must be assumed to be identical for all normal and tumor tissues. However, as shown later [12–16], this is not a good assumption. Thus, the resulting rough estimates cannot be regarded as a representative description of the real, in vivo oxygen supply situation.

Nonetheless, Thomlinson and Gray [11] concluded, after applying estimated critical diffusion distances based on different tissues and tissue geometries, that oxygen depletion (i.e., chronic hypoxia) must be the primary factor leading to the development of necrosis.

This dogma still governs the literature on O_2 supply to tumors, i.e., not considering varying diffusion geometries and other factors at work.[2] For example, the Hill-model postulates there is a *centripetal* diffusion when blood vessels surround the tumor cord. This is in contrast to the Krogh-model which hypothesizes *centrifugal* diffusion when axial blood vessels are surrounded by tumor cords. This geometric difference, whether blood vessels surround or are surrounded by tumor cords, is thus biologically highly significant because, even when being in identical O_2 supply conditions, diffusion that is driven by centrifugal forces alone would lead to 2.7 times larger hypoxic subvolumes and about 25% shorter diffusion distances (data refer to the arterial end of the microvessels) compared to what happens when driven by centripetal diffusion (Fig. 1).

In addition to ignoring diffusion geometries, the impact of glucose, the major nutrient in the development of necrosis, is completely neglected in Thomlinson and Gray's analysis. We return to this point below.

Furthermore, the fact that O_2 diffusion distances progressively decrease in the radial direction from the microvessel into the surrounding tissue, as well as in longitudinal from the arterial to the venous end of the microvessel, is not considered. This results in completely neglecting that the rim of normoxic cells surrounding a patent blood vessel becoming thinner.

Yet there is strong evidence of this phenomenon. For example, data from human melanomas [18] found a thinning from ~ 200 to ~ 20 μm (modal value: 110 μm). Similarly, in human breast cancers, diffusion distances for O_2 decreased from ~ 70 (arterial inflow) to 30 μm (venous outflow) [15, 16]. Oxygen supply distances in human hypopharyngeal cancers (FaDu xenografts) varied between ~ 140 and ~ 40 μm with a median of 80 μm. Within normoxic rims surrounding patent tumor microvessels, unrestricted proliferation of cancer cells occurs. The dimensions of these

[2] There is clear evidence that singular "typical" diffusion distances cannot exist in malignant tumors. Instead, a broad distribution (i.e., a continuum) of O_2 diffusion distances is usually observed [17]. This is expected, due to the longitudinal and radial pO_2 gradients described in this section.

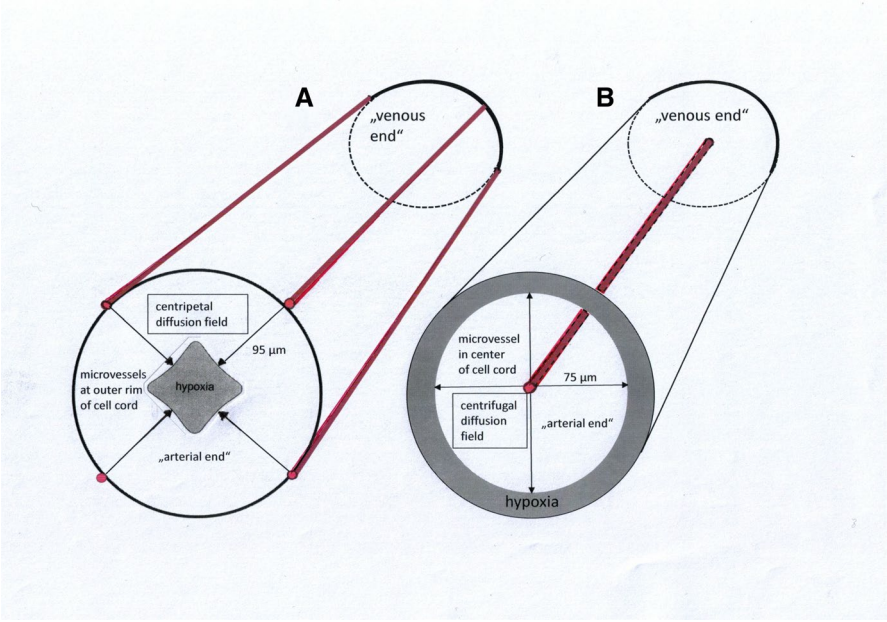

Fig. 1 Centripetal O_2 diffusion with blood vessels surrounding a tissue cord (Hill model, **A**) versus centrifugal diffusion with an axial vessel surrounded by a tissue cord (Krogh model, **B**). The latter diffusion geometry is characterized by shorter diffusion distances (−25%) at identical arterial oxygen availabilities

cone-shaped rims further depend on (a) blood flow directions (concurrent vs. countercurrent blood flow), (b) diffusion shunts in glomerular or chaotic vascular networks and between the inflow limb and outflow limb of hairpin-shaped, countercurrent microvessels, etc.), and (c) variations between different tumor types.

Normoxic tissue cones are surrounded by a variable hypoxic rim, which is adequately supplied with glucose. More specifically, since critical diffusion distances for glucose are about 160 µm (at the arterial end) and approx. < 70 µm (at the venous end of microvessels) in breast cancer, glucose is still available in hypoxic tumor regions. When glucose is used for anaerobic glycolysis in this outer rim, a (reduced) energy supply is still maintained, i.e., at 2 ATPs per mole of glucose, there is an accelerated glycolytic flux by HIF1α- mediated activation of glucose uptake and of key glycolytic enzymes [18]. Therefore, necrotic tissue is found only quite distant from the hypoxic zones where the glucose supply also becomes inadequate.

Figure 2 illustrates the diffusion distances for oxygen (O_2) compared to glucose, showing that glucose (the nutrient needed for functioning) can diffuse much farther than oxygen, allowing cells to survive if they are able to adapt to anoxic conditions. (The data used in Fig. 2 are based on breast cancers.) Note that oxidative metabolism and aerobic glycolysis (i.e., the Warburg effect) are thus restricted to tissue volumes next to the blood vessel and to adjacent areas sufficiently supplied with both O_2 and glucose, whereas anaerobic/hypoxic glycolysis is expected to be occurring in hypoxic/anoxic regions that still exhibit an adequate glucose supply. Having a critical oxygen supply is thus thought to be the

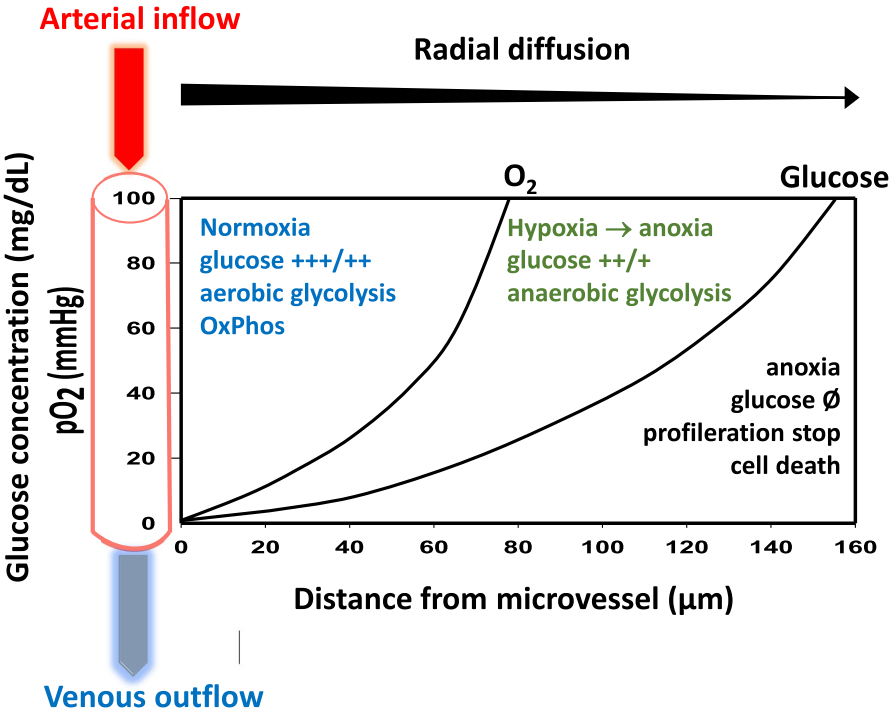

Fig. 2 Relationship between mean critical diffusion distances for oxygen (O_2, left curve) and glucose (right curve). The data shown here, to compute radial diffusion distances from an axial blood vessel within a tissue cord, used in vivo data assessed in xenograft breast cancers. As shown for oxygen diffusion, at the arterial end of the blood vessel ($pO_2 = 100$ mmHg), the critical diffusion distance for oxygen is ~ 75 µm, followed by a fast decline with decreasing blood pO_2 values towards the venous end. The respective critical diffusion distance for glucose at the arterial end of the tumor blood vessel ($c_{gluc} = 100$ mg/dL) is ~ 160 µm, followed by a slightly slower decline with decreasing blood glucose concentrations towards the venous end. This flatter slope is due to a smaller extraction rate for glucose (~ 38%) than for O_2 (~ 44%) [44]. Direction of blood flow is marked by arrows

primary substrate limitation that restricts rapid proliferation, but it is not the critical limitation for cell survival and necrosis formation. Instead, the latter may be attributed to glucose depletion, possibly combined with other detrimental factors. This is in contradistinction to the thesis based on Thomlinson and Gray.

In addition, studies in the late 1990s showed that, since pO_2 values decline more rapidly with distance from blood vessels than do glucose levels, low O_2 levels are the first substrate limitation confronting cancer cells. Consequently, in most malignant tumors, oxygen depletion merely limits cell proliferation rather than causes necrosis [16].

In sum, these more recent data, and especially the more complex understanding regarding the biologically significant pathways that influence diffusion and cellular energy supply, necessitate a major revision of the relationship between hypoxia and necrosis. Several others have noted and agreed with the urgent need

Table 2 Chronic hypoxia in the literature: Synonyms, major causative factors (pathogenesis), and timeframe of exposure

Synonyms of chronic hypoxia	Continuous, diffusion-limited, long-term, sustained, static, steady state
Causative factors	1. Diffusion-limitations
	Enlarged diffusion distances*
	Adverse diffusion geometries* (concurrent vs. countercurrent blood flow, Krogh- vs. Hill-type diffusion geometry)
	Extreme longitudinal intravascular O_2 gradients*
	Shunt perfusion*
	Shunt diffusion
	2. Hypoxemic hypoxia
	Tumor-associated anemia*
	Therapy-induced anemia*
	HbCO formation in heavy smokers
	Small liver tumors supplied by portal vein
	3. Compromised perfusion of microvessels*
	Disturbed Starling forces caused by high interstitial fluid pressure (transmural coupling and drop in perfusion pressure)
	Compression of microvessels caused by solid-phase stress due to non- fluid components
	Intratumor thrombosis
	Long term obstruction of the microvasculature
Timeframe for chronic hypoxia	60 min – weeks

*Groebe and Vaupel [15] reported computed O_2 diffusion radii for these pathogenetic conditions in a human breast cancer cell line

to revise the original (and often misleading) data interpretation by Thomlinson and Gray (which has been commonly accepted for more than 65 years!) [19, 20].

4 Pathogenesis-Related Classifications of Tumor Hypoxia

Understanding the major causative factors (pathogenesis) underlying hypoxia is important because both acute and chronic hypoxia in tumors can contribute to their malignant progression and can impact the efficacy of their treatment.

G. Schwarz, more than 110 years ago, was the first to describe the effect of ischemic hypoxia, a subtype of ***chronic hypoxia***, in protecting from X- and γ-rays [21]. By placing sources of γ-ray on his own arm and binding one source tightly while leaving the other unbound, Schwarz observed that skin compression with its subsequent reduction in skin blood flow negatively influenced the radiosensitivity of cells, i.e., produced less radiation burn. About 65 years ago, Thomlinson and Gray [11] in their influential paper also discussed the phenomenon of diffusion-limited hypoxia, another subtype of chronic hypoxia.

Table 3 Acute hypoxia in the literature: synonyms, major causative factors (pathogenesis), and timeframe of exposure

Synonyms of acute hypoxia	Transient, short-term, perfusion-limited, cyclic, fluctuating, intermittent, periodic
Causative factors	1. Temporary flow stop in microvessels
	Due to tumor cell or blood cell aggregates, fibrin clots
	Ischemic hypoxia due to vascular remodelling
	2. Transient hypoxemia
	Temporary plasma flow in microvessels*
	Fluctuating red blood cell fluxes
	3. Thermoregulation in superficial tumors
Timeframe	Rapid cycles: 2–5 cycles per hour. Slow cycles: Cycles over hours

Groebe and Vaupel [15] reported computed O_2 diffusion radii for these pathogenetic conditions in a human breast cancer cell line

These are but two of the many studies regarding the pathophysiology that explain how chronic hypoxia can lead to poorer prognosis or alter the impact of treatment. The major factors hypothesized in this large body of work, along with the many synonyms for this phenomenon and the timeframes (exposure times) associated with chronic hypoxia are summarized in Table 2. Of interest but not detailed here is the observation of the different stability of HIF-1α and HIF-2α, and the duration of hypoxia [22].

In contrast, regions of ***acute hypoxia*** develop in tumors as a result of short-term interruptions or transient fluctuations in blood flow. The occurrence of acute hypoxia was first described in 1979 by Brown [23] and Yamaura and Matsuzawa [24] and was experimentally evidenced by Chaplin and colleagues in 1987 [25]. Since then, a large body of literature discussing the differing mechanisms that cause acute hypoxia and reporting on their timeframes (exposure times) has been published (see the summary in Table 3).

Later on, Vaupel and Mayer [26] added another relevant pathogenetic factor for the development of tumor hypoxia, i.e., ***hypoxemic hypoxia,*** which may be either chronic (e.g., in tumor-associated or therapy-induced anemia) or acute (e.g., during plasma flow only in the tumor microvasculature).

Other biological factors besides the multiple pathophysiological paths of hypoxia complicate the measurement of hypoxia in tissues. As an example of the problems confounding our understanding of the biology of acute hypoxia, consider the complexity of the subvolumes in normal and tumor tissues. Unfortunately, hypoxic subvolumes/subregions are often organized on a submillimeter scale with steep gradients between well-oxygenated and hypoxic regions [17]. Therefore, the spatial resolution of hypoxia imaging is too low with regard to observing the spatial dimensions of the microregional heterogeneities.

Furthermore, cyclic variations in tumor oxygenation have been observed on timescales that are substantially shorter than the 1–2 h post bolus injection in typical PET studies. For example, radial diffusion times of misonidazole, [^{18}F]Fluorodeoxyglucose

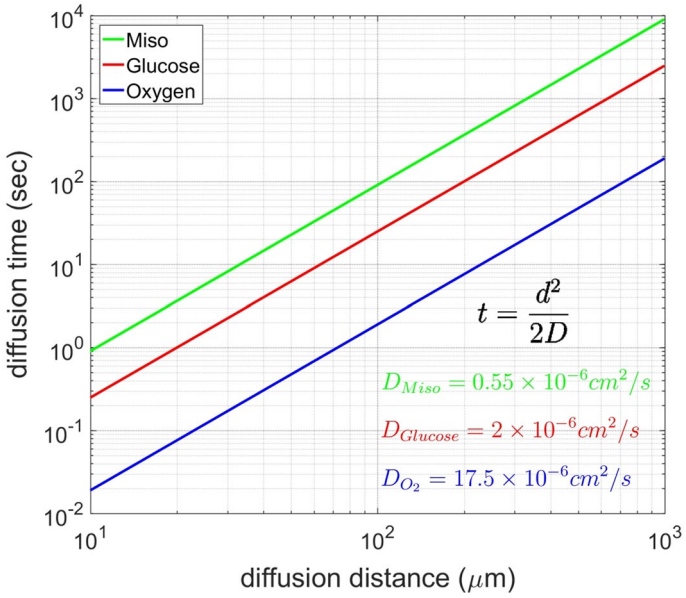

Fig. 3 Diffusion times for oxygen, glucose and misonidazole (exogeneous hypoxia marker) in tumor tissues (based on Einstein's diffusion equation, D = diffusion coefficient in tumor tissue)

and oxygen within tumor tissues, calculated using Einstein's equation for one-dimensional diffusion can occur within seconds or minutes, as shown in Fig. 3. Since maximum distances between adequately perfused microvessels can exceed 1 mm in cancers [27], the diffusion time for O_2 is expected to be about 1 min to reach central microareas between the microvessels. For glucose, the diffusion time is ~ 10 times, and for misonidazole almost 40 times longer [28]. These long diffusion times may prevent capturing the signal of fast changes. To date, the diffusion limitations of PET tracers to hypoxic regions may lead to (a) low-signal-to-noise ratios (i.e., poor accuracy) or (b) complete failure to detect acute hypoxia in the clinical setting (i.e., incorrect clinical interpretation of the presence/absence of hypoxia).

Despite the considerable effort that has been devoted by many laboratories and researchers in trying to understand the mechanisms and measures of acute and chronic hypoxia, these studies have not yet resulted in reaching an understanding of tumor biology that is sufficient for designing novel treatment strategies, for detecting tumors by imaging and for targeting tumor treatments in personalized medicine [26, 29, 30].

5 Direct Assessment of the Oxygenation Status and Detection of Tumor Hypoxia using pO_2 Polarography

Direct assessment of the tumor oxygenation status using polarography in experimental tumors and in the clinical setting dates back to the late 1950s, i.e., Urbach's studies of pO_2 values in human skin tumors [31, 32] and to the early 1960s using various invasive techniques.

To date, the most direct and frequently used method to describe tissue oxygenation is polarographic measurement of O_2 partial pressures (pO_2 tensions).[3] With this (ideally) minimally invasive microtechnique, frequency distributions (histograms) of measured intratumor pO_2 values are assessed with a high spatial resolution. Other direct procedures used in the clinical setting include fiberoptic sensors and electron paramagnetic resonance (EPR) oximetry, the latter method also being minimally invasive, requires only application of the paramagnetic material. (EPR studies have been discussed in Swartz et al. [8] and Schaner et al. [36]).

Anecdotal and sporadic reports of the pO_2 distribution in animal and human tumors are all based on polarographic measurements (for a review see [37]). These experiments already provided some hints that hypoxia and anoxia may occur in malignant tumors at advanced growth states due to the surpassing of critical supply conditions.

The development, applicability, and clinical impact of pO_2 microsensors in oncological research to assess the oxygenation status of tumors and to investigate the sophisticated pathogenesis of tumor hypoxia, a key hallmark of cancers, is roughly outlined in Table 4.

5.1 Oxygenation Status of Isograft Tumors

The first systematic studies on isograft rat tumors were performed by Vaupel et al., starting more than 50 years ago, using self-made, membrane-covered gold

[3] Directly measured tumor pO_2 values using oxygen electrodes, data derived from hypoxia imaging procedures, the expression of hypoxia-inducible biomarkers and the detection of exogeneous compounds have been correlated, although these different techniques assess hypoxia on different scales.

In *imaging studies* (a) the spatial resolution was often too low with regard to the spatial dimension of microregional heterogeneities, and (b) different biologically relevant levels of hypoxia could not be discriminated, thus excluding correlations with oxygen electrode measurements, and (c) adequate tracer accumulation may be inadequate due to long diffusion times, as mentioned in Sect. 4.

Endogenous biomarkers cannot substitute for direct pO_2 measurements mainly since the expression of HIF-1α and its downstream proteins (e.g., GLUT 1, CA IX) are significantly modulated by non-hypoxic signaling (e.g., in Warburg phenotypes). In addition, in many studies the biomarker expression was detected in tumor subregions distant from the region of the electrode track, thus excluding any correlation [33–35].

In hypoxia detection with *exogenous bioreductive compounds,* no clear correlations were found between pO_2 measurements and tracer uptake. Major reasons for this missing correlation may be (a) long diffusion times and (b) comparing tumor microregions from different tumor subvolumes [6].

Note: Immunohistochemical biomarker detection and pO_2 readings must be derived from identical tumor subvolumes / tumor regions. Otherwise, correlation analyses based on these two data sets are not appropriate.

Table 4 Assessment of the tumor oxygenation status using pO_2 polarographic microsensors, hypoxia detection, and first description of the association between tumor hypoxia, malignant progression and poor patient prognosis: A remarkable preclinical and clinical research history

Timetable	Cornerstones	First publications
Since early 1940s	Continuous development of microelectrodes for the measurement of local pO_2 values in living tissues	[132, 133]
Late 1950s	Start of anecdotal and sporadic measurements in human tumors in situ	[31, 32]
Since early 1970s	Systematic pO_2 studies on isograft rat and mouse tumors. Evaluations of the pathogenesis of tumor hypoxia	[38]
	Mathematical analyses of critical O_2 diffusion distances in tumors using in vivo-data	[40]
Since mid-1980s	Systematic studies on xenograft human tumors in vivo	[134]
	First observation of a causal relationship between moderate hypoxia ($pO_2 < 8$ mmHg) in *lymph node metastases* of head and neck cancers and response to radiotherapy	[48]
Since late 1980s	Systematic studies on human primary and recurrent cancers in situ (breast, cervix and vulva cancers)	[53, 54, 56]
	In the following years, pretherapeutic hypoxia (with pronounced heterogeneities within and between tumors, and different severities of hypoxia) could be detected in a multitude of malignancies	
1992	*As a note*: Discovery of the hypoxia-induced transcription factor HIF-1, which promotes changes in the transcriptome and proteome of moderately hypoxic tissues, malignant tumors included	[62]
Since early 1990s	pO_2 histography system considered the "gold standard" for detection of microregional hypoxia	[55]
	Experimental proof for the existence of steep pO_2 gradients on a sub-millimeter scale	[53]
Since 1993	Pretherapeutic hypoxia, a hallmark of most cancers, is a strong, independent and adverse prognostic factor of *primary cancers* favoring malignant progression and poor patient prognosis. Tumor hypoxia ($pO_2 < 10$ mmHg) is associated with resistance to antitumor therapies (e.g., radiotherapy, some chemotherapy, immunotherapy)	[60, 61]

microelectrodes with tip diameters of 1–8 µm [38, 39]. These experiments showed that (a) tumor oxygenation is extremely heterogeneous and (b) the pO_2-histograms (i.e., pO_2-distribution curves) were extremely left-shifted, i.e., most values of pO_2 were very low and the median pO_2 exponentially decreased from 6 to 3 mmHg with increasing tumor volume. As early as 1974, Vaupel and Thews [40] theoretically analyzed the critical O_2 supply conditions in tumor tissues. Their work was based on experimental data, on diffusion equations using in vivo data, and on measured O_2 diffusion coefficients of tumor tissues (having a 10% higher water content than normal soft tissues). Their results suggested two causal mechanisms for severe hypoxia developing with increasing tumor size: *diffusion-limitations* (due to increasing intercapillary distances and lengths of tumor microvessels) and *perfusion-limitations* (as a consequence of an exponential drop of the size of the vascular space).

This was the first description differentiating between diffusion-limited and perfusion- limited chronic hypoxia. In addition, their initial estimates (detailed below) clearly showed that isobaric inspiratory hyperoxia and arterial hyperoxemia ($pO_2 > 450$ mmHg) can only improve the O_2 supply at the arterial end of the tumor microvessels. The peripheral areas, especially at the venous end of the microvessels are not influenced at all [40].

There were two sets of initial findings that led to these observations: O_2 partial pressures measured in isograft C3H mouse breast cancer using "gold in glass" type microelectrodes with tip diameters of 1–5 µm -in principle- revealed similar results: The median pO_2 was 4 mmHg, the modal class being 0–5 mmHg. Here again, the mean pO_2 values exponentially decreased with increasing tumor volume from about 10 mmHg to 2 mmHg. Pronounced heterogeneities existed within the same tumor considering different microelectrode tracks. Left-shifts of the pO_2-distribution curve toward having mostly very low values were a common finding [41].

Computer-based analysis of the spatial distribution of intratumor pO_2 values assessed with the pO_2- histography system, originally described by Weiss and Fleckenstein [42], was possible by interpolating the measured pO_2 values in different tumor layers using an inverse-distance weighting algorithm [43]. Data confirmed that the spatial pO_2 distribution is chaotic and anisotropic: In small tumors, large areas with relatively high pO_2 values were identified next to small confluent hypoxic areas. With increasing tumor volume, the spatial distribution became more uniform with a preponderance of low pO_2 values (see Fig. 4).

5.2 Oxygenation Status of Human Tumor Xenografts

In the mid-1980s, tissue oxygenation in human breast cancer xenografts grown in immune-deficient rats was assessed using recessed, membrane-covered Whalen-type, self-made O_2-sensitive microelectrodes with tip diameters < 20 µm. In general, there was a distinct shift of the pO_2-distribution toward lower values with increasing tumor volumes similar to those described for isograft tumors. Besides intratumor heterogeneities, there was a marked inter-tumors variability with severe hypoxia existing between neighboring microregions [44].

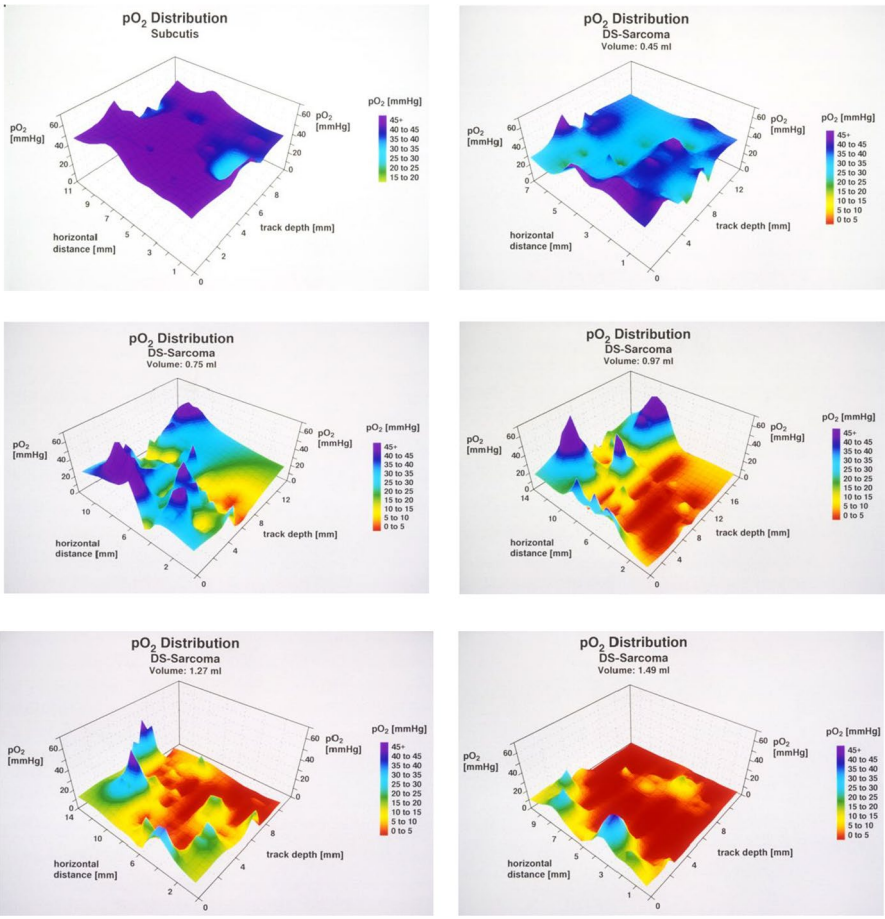

Fig. 4 Reconstructed spatial pO_2 distributions in the lower, horizontal tissue layer of the normal subcutis and of isograft tumors with increasing volumes from 0.45 to 1.49 ml. Computation based on polarographic pO_2 measurements (O. Thews and P. Vaupel, unpublished data)

pO_2 measurements were also performed in a large number of human tumor xenografts with greatly differing blood flow rates using a prototype of the Eppendorf histography system. This was available for the first time in the mid-1980s in our laboratory [45, 46]. Considering O_2 levels in well-perfused tumors as a function of volume, a worsening of the tissue oxygenation status was noted in advanced growth states, concomitant with a decrease of tumor blood flow rates. Hypoxic subvolumes in these well-perfused xenografts were $< 10\%$ of the measured total volume. In contrast, in poorly perfused tumors, hypoxia ($pO_2 < 5$ mmHg) was already detected in $> 50\%$ of the tissue mass at much smaller volumes. There was clear evidence that the median/mean pO_2 strongly depended on the O_2 availability, and thus on the efficacy of tumor blood flow.

5.3 Oxygenation Status and Hypoxia Detection in Human Tumors in Situ

As already mentioned, anectodal and sporadic pO_2 measurements in human tumors date back to the late 1950s and early 1960s, and have been reviewed earlier (e.g., [47]). Nearly two decades later, Gatenby et al. [48] described a polarographic technique that, using CT- guided probes, allowed in vivo mapping of tumor oxygen levels in *lymph node metastases* of head and neck cancers (SCCHN). Our preceding studies, using a cryospectrophotometric approach on tumor cryobiopsies, published for isograft and xenograft tumors and for human primary carcinomas of the oral cavity [49] and of the rectum [50], i.e., "lowered oxygen levels and nonrandom distributions", were thus confirmed. Later, Gatenby et al. [51], defining a pO_2 cutoff of 8 mmHg, described a relationship between pO_2 in *lymph node metastases* of SCCHN and responses to radiotherapy.

Systematic studies in the clinical setting on *primary and recurrent gynecological cancers* (breast, uterine cervix, vulva) were initiated in the late 1980s by the Höckel/Vaupel group using the Eppendorf pO_2 histography system. As commended by G. Semenza, Nobel Prize Winner of Physiology or Medicine in 2019, these "groundbreaking clinical studies" [52] were expanded by correlation analyses of measured pO_2 values and expression of endogenous hypoxia markers in the Vaupel/Mayer laboratory [33–35].

Prerequisites for these latter coexistence analyses were needle core biopsies immediately after the pO_2 measurements. These core biopsies, including the tumor subvolume around the microsensor track, also allowed exclusions of pO_2 measurements in necrotic regions [33]. Without this exclusion, our thesis that tumor hypoxia may have a strong impact on patient survival could not have been validated in a prospective study (see Sect. 5.3.3).

5.3.1 The Computerized pO_2 Histography System for Direct Assessment of Tissue Oxygen Tensions

This novel system was tested and validated in the late 1980s under in vitro and in vivo conditions before starting its use in the clinical setting. The histography system was found to be reliable in isotonic solutions and in fresh donor blood. Histograms obtained in rat liver, mouse skeletal muscle, and subcutis were comparable with previously reported pO_2 distributions obtained using Whalen-type microsensors [44]. The measuring micro-cathode, imbedded in a jacket tube, was mechanically stable and only had a negligible O_2 consumption and did not exert compression artifacts (as evidenced by lacking negative pO_2 readings) due to the special stepwise forward movement immediately followed by a backward step of 30% of the forward movement. Details of the measuring system were repeatedly and comprehensively described (e.g., Vaupel et al. [53, 54]). A critical evaluation of the computerized pO_2 histography system, approved for clinical use and considered to be the gold standard for microregional hypoxia detection since the early 1990s has been summarized in a meeting report by Tatum et al. [55]. Despite some limitations due primarily to its invasive nature and to some variations associated with operator use, the system was successfully used to assess oxygen levels in tissues in 30 institutions (22 in Europe, 5

in the USA, 2 in Canada, and 1 in Australia). Altogether, hypoxia detection was possible in 15 different tumor entities (primary, recurrent, metastatic, benign tumors), mainly in accessible SCCHNs, breast cancers, cervix cancers, soft tissue sarcomas and primary brain tumors (for a comprehensive overview see [54]).

The prognostic significance of pretherapeutic tumor hypoxia was validated by multivariate analyses for cancers of the uterine cervix (using disease-free survival [DFS]), for SCCHNs (overall survival [OS], local control [LC]) and soft tissue sarcomas (DFS, OS, distant spread).

The grand median pO_2 value in these investigations was ~ 10 mmHg, i.e., all tumors were moderately/severely hypoxic before therapy. The hypoxic fraction with pO_2 values ≤ 2.5 mmHg in these tumors was about 20%. (In normal tissues pO_2 values ≤ 2.5 mmHg have been detected only in the inner medulla of the kidney, HF2.5 = ~ 10%, and in the uterine cervix, HF2.5 = ~ 8%). Pancreatic adenocarcinomas ($n = 8$) were the most hypoxic cancers as evidenced by a hypoxic fraction HF2.5 of ~ 60% and a median pO_2 of 2 mmHg.

Although the computerized pO_2 histography system, equipped with a recessed tip microelectrode, provided biologically relevant information and the most detailed data with prognostic power in the clinical setting so far, this technique, although found to be reliable, is no longer commercially available because the invasive nature of this method limited its broader clinical application.

5.3.2 Hallmarks of Human Cancer Oxygenation

The Höckel/Vaupel group focused on locally advanced gynecological cancers [53, 56, 57]. For comparison, they investigated the oxygenation status of selected non-malignant pathologies (e.g., fibrocystic breast disease, uterine fibroids) and normal tissues.

Accumulated evidence has shown that most *primary cancers* may exhibit hypoxic and anoxic tissue subregions that are heterogeneously distributed within the tumor mass. The pretherapeutic oxygenation status assessed in breast, cervix, and vulva cancers was poorer than that in the respective normal tissues and is independent of clinical size, stage, histology, grade, nodal status, and a series of other tumor characteristics or patient demographics. Furthermore, results obtained on primary cancers do not suggest a topological distribution of pO_2 values within a tumor (e.g., center versus tumor periphery). They also show that tumor-to-tumor variability in oxygenation is greater than intratumor variability.

Local *recurrences* have a higher hypoxic fraction than the respective primary tumors [58]. The findings that hypoxic subregions in *metastases* are larger than in the primaries are not always consistent. Cancers in *anemic patients* are more hypoxic (i.e., anemic hypoxia) than in non-anemic patients [59]. Heterogeneities in the oxygenation status exist on a microscopic scale as evidenced by immunohistochemistry and steep pO_2 gradients have been described (e.g., 40–50 mmHg/mm).

Transgression of grade IVA cervix cancers into neighboring tissues can have an impact on the pretherapeutic oxygenation status due to parasitic connections to the surrounding vascular networks (i.e., "vascular co-option" by incorporation of preexisting vessels into the invading tumor).

5.3.3 Tumor Hypoxia, Prognostic Value and Adverse Impact on Clinical Outcome

The Höckel/Vaupel group [60, 61] was the first to describe the association between tumor hypoxia ($pO_2 < 10$ mmHg) and poor prognosis in primary carcinomas. This knowledge coincided with three important explorations supporting the hypothesis that hypoxia was associated with malignant progression and poor patient prognosis: (a) the exploration of the molecular basis of hypoxia-induced genome changes associated with malignant progression, (b) the discovery of the hypoxia-inducible factor (HIF) (triggering changes of the tumor proteome [62, 63]), and (c) consideration of the roles of clonal selection (mechanisms described in the early 2000s, e.g., [64–66]).

Tumor hypoxia has also been classically associated with acquired treatment resistance (radiotherapy with X- and γ-rays, numerous chemotherapeutic agents, immunotherapy, and photodynamic therapy) [7].

6 4D-Heterogeneity of O_2 Partial Pressures (pO_2 Values) in Malignant Tumors: Reference Data Based on Direct Measurements

The realization that hypoxia (i.e., a critically reduced oxygenation status) is a major hallmark of cancer and a key driver of malignant progression requires an exact, updated knowledge of the oxygenation status of solid malignancies (see Table 5), especially because a series of inconsistencies and fallacies are often encountered in the description of tumor hypoxia, e.g., incorrect units, basic conceptions of respiratory physiology not considered, equivocal (and without any need) conversion of partial pressures into concentrations in heterogeneous tissues without knowledge of the solubility coefficient α, and inadequate terminology.

7 Physiological Variability of O_2 Partial Pressures (pO_2 Values) in Normal Tissues/Organs: Updated Reference Data Obtained from Direct Measurements

While the characteristic ***spatio-temporal heterogeneities*** *("chaotic 4D- heterogeneities")* within and between tumors of the same type, size and grade are mainly caused by pathophysiological mechanisms ("pathomechanisms") occurring during carcinogenesis and unrestricted growth, the ***structurally and physiologically organized variability*** in normal tissues/organs is based on various morphological, functional, metabolic, tissue-specific features.

As shown in Table 6, tissue oxygen levels in healthy individuals may vary due to (a) zonal structures (e.g., liver), (b) compartmentations within organs and tissues (e.g., eye, bone), (c) age-related changes (e.g., thymus), (d) different morphologies with special functions (e.g., brain, kidney), (e) existence of different tissue subtypes and their individual functions (e.g., white and brown adipose tissue), (f) adjacent tissue layers with specific functions (e.g., epidermis and dermis involved in thermoregulation), (g) organs that have a specific microvascular organization (e.g., closed

Table 5 Pretherapeutic oxygenation status of human tumors, assessed by the pO_2 histography system

Tumor type (ordered by no. of patients)	No. of patients	Grand median pO_2 (mmHg)	HF2.5 (%)	pO_2 range (mmHg)	Prognostic significance of tumor hypoxia	References
Cervix cancers	730	10	28	0–88	DFS, OS, DS	For reviews see [7, 8, 54]
Primary	177	12				[58]
Recurrent	53	7				[58]
Anemic	19	6				[59]
Head and neck cancers	592	10	21	0–90	OS, LC	For reviews see [7, 8, 54, 70]
Primary		14				[71]
Metastatic		7				[72]
Anemic		7				[72]
Prostate cancers	438	7	26	0–95		For reviews see [7, 8, 54, 73, 74]
Soft tissue sarcomas	283	14	13	0–96	DFS, OS, DS	For reviews see [7, 8, 54]
Recurrencies	11	20	12	0–95		[75]
Breast cancers	212	10	30	0–95		For reviews see [7, 8, 54]
With stromal compartment	15	28	4	0–95		[76]
Non-anemic	18	10				[77]
Anemic	11	4				[78]
Benign breast tumors	12	45	2	0–95		[79]
Glioblastomas	104	13	26	0–50		For reviews see [7, 8, 54]
Vulvar cancers	54	11	25	0–92		For reviews see [7, 8, 54]
Primary	15	13				[57, 59, 80]
Recurrent	19	11				[57, 80]
Anemic	8	5				[59]
Rectal cancers, primary	29	25	n.a	0–92		[81–83]
Metastatic (liver)[#]	4	6	n.a	0–92		
Recurrencies	5	8	28	0–80		[75]
Lung cancers	26	16	13	0–95		[84, 85], for reviews see [7, 54]

Table 5 (continued)

Tumor type (ordered by no. of patients)	No. of patients	Grand median pO_2 (mmHg)	HF2.5 (%)	pO_2 range (mmHg)	Prognostic significance of tumor hypoxia	References
Malignant melanoma (metastases)	18	12	5	0–96		[86]
Non-Hodgkin's lymphomas	8	18	36	0–92		[87]
Pancreas cancers	8	2	59	0–91		[88, 89]
Brain metastases	5	10	26	0–87		[90]
Renal cell carcinomas	3	10	n.a	0–90		[91]
Gall bladder cancers	1	4	n.a	0–10		[89]
Bile duct cancers	1	8	n.a	0–15		[89]

1 mmHg = 0.133 kPa; DFS: disease-free survival, OS: overall survival; LC: local control; DS: distant spread; n.a.: data not available. # Reliable pO_2 data for hepatocellular carcinomas are not available (~2021)

Table 6 Oxygen partial pressures directly assessed with polarographic pO_2 microsensors or fluorescence-based microsensors in human tissues and organs ($FIO_2 = 0.21\%$, resting and ambient temperature conditions)

Organ, tissue	Grand mean pO_2 [mmHg]	Remarks	References
1. Respiratory system			
Inspired air	156	At sea level	
Tracheal lumen	145–150	Moist air	
Bronchial lumen	115–145		
Alveolar space	100–109		
Lung parenchyma	43	Peribronchial tissue	[94, 95]
Carotid bodies			
Outer layers	68	0–15 mmHg (controversial data, Acker et al. [96])	[97]
Deeper layers	42	25–90 mmHg (controversial data, Acker et al. [96])	
2. Cardiovascular system			
Arterial blood	77–98 (at rest)	Progressive decrease with age	[94, 98]
Mixed venous blood	~ 40		[94]
Aortic wall	~52		[99]
Luminal layers	70–75	pO_2 decline upon long-term hypertension	
Media (central)	20–25		
Adventitia	55–55		
Myocardium	16–25		[100–102]
Subepicardial	18–26		
Subendocardial	10–17		
3. Feto—maternal unit			
Umbilical vein	~30	Measurements at term/delivery (blood gas analyses together with pH and pCO_2)	[103]
Umbilical artery	~19		
Intervillous space (placenta)	~50		
Uterine artery	98		
Uterine vein	33		

Table 6 (continued)

Organ, tissue	Grand mean pO_2 [mmHg]	Remarks	References
4. Skin, subcutis and breast			
Skin	25–35	Zonal differences	
Critical limb ischemia	5–8		[104]
Limbs venous diseases	15		[104]
Epidermis	8		[105]
Subepidermal layer	35		[105]
	~35	Skin surface temperature: ~33 °C	Vaupel and Thomsen (unpublished)
	~50	Skin surface temperature: ~40 °C	
Dermis	45–55		[106]
Deep dermis/subcutis	42–44	Skin surface temperature: ~34 °C	Vaupel and Thomsen (unpublished)
	~80	Skin surface temperature: ~40.5 °C (rising pO_2 with increasing dermal depth)	
Postoperative healing of skin wounds	32	2 days after abdominal surgery	[107]
	35	10 days after abdominal surgery	
Subcutis	38–47		
Pubic region	52–55		[56]
Abdominal wall (lean vs. obese)	54 vs. 43	Conflicting results with different techniques (summarized by [108])	
Upper arm (lean vs. obese)	54 vs. 47		
Breast	65		[53, 76]
Fibrocystic disease	67		[53]
5. White adipose tissue			
Lean persons	54	Conflicting results with different techniques (reviewed by [108])	[109–112]
Obese persons	43		

Table 6 (continued)

Organ, tissue	Grand mean pO_2 [mmHg]	Remarks	References
6. Urinary system			
Kidney	31	Zonal differences (functional differences)	[91]
Superficial Outer Cortex vs. Cortex	70 vs. 50		[113]
Glomerulus	~55		[114]
Outer medulla	38		[113]
Inner medulla	10–15	Hypoxic fraction ≤ 2.5 mmHg: ~10%	[115]
Urinary bladder wall	43		[116]
7. Endocrine system			
Islets of Langerhans (pancreas)	40–45		[117]
Suprarenal glands	55		[93]
8. Gastro-intestinal tract			
Intestinal tissue	58	Different anatomical and functional entities	[92, 94]
Mucosa, oral	52		
Gastric	55–60	*Luminal* pO_2 decline along the length of the GI-tract; EPR technique [94]	[118]
Small bowel	61		
Large bowel	58		
Rectum	51		[82]
9. Upper abdominal organs			
Pancreas, exocrine	30–40		[94, 119, 120]
Liver	30–40	Zonal differences with differences in functions	[82, 94, 121]
Periportal zone	45–50		
Centrilobar zone	15–20		
Spleen	68	Organ with open and closed circulation Aspiration, blood gas analyses	[122]

Table 6 (continued)

Organ, tissue	Grand mean pO_2 [mmHg]	Remarks	References
10. Reproductive system			
Uterus, lumen	15–20		[94]
Myometrium	10–20	HF2.5 = 5%	[123]
Cervix	~40	HF2.5 = 5–10%	[58]
Leiomyoma	1	HF2.5 = 73% (Immunohistochemistry: HIF-negative !)	[123]
Prostate	26		[74]
11. Skeleton, skeletal muscle			
Bone, cortical	31		[124]
Hematopoietic marrow	22–54	Blood gas analyses after aspiration	[94]
Adipose marrow	26		
Periosteum	15–45		
Articular cartilage	~10		
Synovial fluid	10–45		
Skeletal muscle, resting	27–32	HF2.5 = 5–10%	[98]
Exercise	~10	HF2.5 = 40%	[125]
Hypovolemic shock	4	HF2.5 = ~ 30%	[104]
PAOD	6–7	PAOD = peripheral art. occlusive disease	[126]
12. Brain			
Gray matter	28–36	Zonal differences with different functions	[94, 127, 128]
Occlusion of cerebral artery	≤ 5	Mean pO_2 decreases with brain depth	
White matter	10–15		
Hypothalamus	10–15		
Midbrain	5		
Pons	2–3		

Table 6 (continued)

Organ, tissue	Grand mean pO_2 [mmHg]	Remarks	References
13. Eye			
Choroid	60	Functional compartments with different functions	[129, 130]
Vitreous humor	15–25		
Choroid-retinal border (relative depth = 100%), outer retina	60		
Vitreo-retinal border (relative depth = 0%), inner retina	15–25	pO_2 changes with differing physiological functions (e.g., light vs. dark adaptations)	
pO_2 sink at retina depth of 70–80%	0–10		
Lens	25–65		[131]
Aqueus humor	~70		
Cornea	125–30		
Lacrimal fluid	~130		

Updated human data, whenever available. pO_2 is the driving force for O_2 diffusion in the body. For earlier reviews see [8, 92–94]

vs. open circulation in the spleen), (h) tissues with dual, diffusive *and* convective, oxygen supply (e.g., skin), (i) hollow organs exposed to varying wall tensions (e.g., heart, aortic wall, urinary bladder), and (j) temporary, rapidly growing organ systems (e.g., fetal-placental unit). Note: It should be pointed out—as mentioned earlier in this article—that the oxygen extraction rate is a major determinant of the actual tissue oxygenation as already described for tumors (see Sect. 2). The "physiological" oxygenation status of the carotid bodies—as evidenced by a grand mean pO_2 of 32 mmHg [67, 68]—results from a blood flow rate of 14.2 ml/g/min (the highest flow rate for any organ in the body! [69]) and a very low O_2 extraction fraction of 0.01; (for comparison, see other O_2 extraction fractions: kidney = 0.1, brain = 0.4 and skeletal muscle = 0.6).

8 Conclusions

The use of the pO_2 histography system in the clinical setting, if properly applied by experienced investigators (e.g., exclusion of pO_2 measurements in grossly necrotic regions and/or in the stromal components of carcinomas, avoidance of "negative" pO_2 readings as a consequence of tissue compression) has unequivocally shown that hypoxia is a chief hallmark of most malignancies in adults. Clinical investigations have detected hypoxic subvolumes which are heterogeneous in (a) extensions, (b) spatial distributions within a tumor, (c) over time, (d) severity (extent), and (e) as a consequence of treatment. Tumor hypoxia ($pO_2 < 10$ mmHg) has been identified as a strong, independent and adverse prognostic factor of several malignancies, leading to poor long-term prognosis in cancer patients [54].

In addition, the pO_2 histography system has enabled us to define an "optimal" hemoglobin concentration with regard to tumor oxygenation, avoiding hypoxemic hypoxia on the one hand and inappropriate treatments/corrections on the other hand [59].

Author Contributions The first draft of the manuscript was written by Peter Vaupel, and all authors contributed to subsequent versions of the manuscript. All authors read and approved the final manuscript.

Funding Open Access funding enabled and organized by Projekt DEAL. None.

Declarations

Conflict of interest The authors declare that they have no conflict of interest.

References

1. M. Höckel, P. Vaupel, J. Natl. Cancer Inst. **93**, 266 (2001)
2. P. Vaupel, G. Multhoff, Adv. Exp. Med. Biol. **1232**, 169 (2020)
3. P. Vaupel, L. Harrison, Oncologist **9**(Suppl. 5), 4 (2004)
4. P. Vaupel, A. Mayer, M. Höckel, Methods Enzymol. **381**, 335 (2004)
5. P. Vaupel, Oncologist **9**(Suppl. 5), 10 (2004)
6. P. Vaupel, A. Mayer, Cancer Metastasis Rev. **26**, 225 (2007)
7. S. Osinsky, H. Friess, P. Vaupel, Tumor Hypoxia in the Clinical Setting (Akademperiodyka, Kiev, 2011). ISBN 978–966–360–169–4
8. H.M. Swartz, A.B. Flood, P.E. Schaner et al., Physiol. Rep. **8**(15), e14541 (2020)
9. A. Mayer, P. Vaupel, Adv. Exp. Med. Biol. **789**, 203 (2013)
10. P. Vaupel, O. Thews, D.K. Kelleher, M.A. Konerding, Int. J. Oncol. **22**, 795 (2003)
11. R.H. Thomlinson, L.H. Gray, Br. J. Cancer **9**, 539 (1955)
12. I. Tannock, Adv. Exp. Med. Biol. **75**, 597 (1976)
13. I.F. Tannock, Br. J. Cancer **22**, 258 (1968)
14. I.F. Tannock, I. Kopelyan, Cancer Res. **46**, 3105 (1986)
15. K. Groebe, P. Vaupel, Int. J. Radiat. Oncol. Biol. Phys. **15**, 691 (1988)
16. P. Vaupel, Strahlenther. Onkol. **166**, 377 (1990)
17. P. Vaupel, A. Mayer, Adv. Exp. Med. Biol. **977**, 91 (2017)
18. P. Vaupel, A. Mayer, H. Schmidberger, Int. J. Radiat. Biol. **95**, 912 (2019). https://doi.org/10.1080/09553002.2019.1589653
19. R.A. Gatenby, R.J. Gillies, Nat. Rev. Cancer **4**, 891 (2004)
20. Q. Wang, P. Vaupel, S.I. Ziegler, K. Shi, Phys. Med. Biol. **60**, 2547 (2015)
21. G. Schwarz, Münch. Med. Wschr. **24**, 1 (1909)
22. K. Saxena, M.K. Jolly, Biomolecul. **9**, 339 (2019)
23. M. Brown, Br. J. Radiol. **52**, 650 (1979)
24. H. Yamaura, T. Matsuzawa, Int. J. Radiat. Biol. Relat. Stud. Phys. Chem. Med. **35**, 201 (1979)
25. D.J. Chaplin, P.L. Olive, R.E. Durand, Cancer Res. **47**, 597 (1987)
26. P. Vaupel, A. Mayer, J. Innov. Opt. Health Sci. **7**, 1330005 (2014)
27. M.A. Konerding, E. Fait, A. Gaumann, Br. J. Cancer **84**, 1354 (2001)
28. P. Vaupel, K. Shi, A. Mayer, Strahlenther. Onkol. **194**(Suppl. 1), 94 (2018)
29. C. Bayer, K. Shi, S.T. Astner, C.A. Maftei, P. Vaupel, Int. J. Radiat. Oncol. Biol. Phys. **80**, 965 (2011)
30. C. Bayer, P. Vaupel, Strahlenther. Onkol. **188**, 616 (2012)
31. F. Urbach, Proc. Soc. Exp. Biol. (N. Y.) **92**, 644 (1956)
32. F. Urbach, Proc. Am. Assoc. Cancer Res. **2**, 154 (1956)
33. A. Mayer, A. Wree, M. Höckel, C. Leo, H. Pilch, P. Vaupel, Cancer Res. **64**, 5876 (2004)
34. A. Mayer, M. Höckel, A. Wree, P. Vaupel, Clin. Cancer Res. **11**, 2768 (2005)
35. A. Mayer, M. Höckel, P. Vaupel, Clin. Cancer Res. **11**, 7220 (2005)
36. P.E. Schaner, J.R. Pettus, A.B. Flood et al., Front. Oncol. **10**, 572060 (2020). https://doi.org/10.3389/fonc2020.572060
37. P. Vaupel, Microvasc. Res. **13**, 399 (1977)
38. P. Vaupel, H. Günther, W. Erdmann, S. Kunke, G. Thews, Verh. Dtsch. Ges. Inn. Med. **78**, 133 (1972). https://doi.org/10.1007/978-3-642-85448-4_22
39. H. Günther, P. Vaupel, H. Metzger, G. Thews, Zschr. Krebsforsch. **77**, 26 (1972)
40. P. Vaupel, G. Thews, Oncology **30**, 375 (1974)
41. P.W. Vaupel, S. Frinak, H.I. Bicher, Cancer Res. **41**, 2008 (1981)
42. C. Weiss, W. Fleckenstein, In: Funktionsanalyse biologischer Systeme **15**, 155 (1986). Eds.: J.Grote, G.Thews Stuttgart: Steiner. ISBN 3–515–04691–7
43. O. Thews, P. Vaupel, Strahlenther. Onkol. **191**, 875 (2015)
44. P. Vaupel, H.P. Fortmeyer, S. Runkel, F. Kallinowski, Cancer Res. **47**, 3496 (1987)
45. F. Kallinowski, R. Zander, M. Höckel, P. Vaupel, Int. J. Radiat. Oncol. Biol. Phys. Med. **19**, 953 (1990)
46. F. Kallinowski, K.H. Schlenger, S. Runkel, M. Kloes, M. Stohrer, P. Okunieff, P. Vaupel, Cancer Res. **49**, 3759 (1989)
47. P. Vaupel, F. Kallinowski, P. Okunieff, Cancer Res. **49**, 6449 (1989)

48. R.A. Gatenby, L.R. Coia, M.P. Richter, H. Kalz, P.J. Moldofsky, P. Engstrom, D.Q. Brown, R. Brookland, G.J. Broder, Radiology **156**, 211 (1985)
49. W. Mueller-Klieser, P. Vaupel, R. Manz, R. Schmidseder, Int. J. Radiat. Oncol. Biol. Phys. **7**, 1397 (1981)
50. P. Wendling, R. Manz, G. Thews, P. Vaupel, Adv. Exp. Med. Biol. **180**, 293 (1984)
51. R.A. Gatenby, H.B. Kessler, J.S. Rosenblum et al., Int. J. Radiat. Oncol. Biol. Phys. **14**, 831 (1988)
52. G.L. Semenza, Biochim. Biophys. Acta **1863**, 382 (2016)
53. P. Vaupel, K. Schlenger, C. Knoop, M. Höckel, Cancer Res. **51**, 3316 (1991)
54. P. Vaupel, M. Höckel, A. Mayer, Antioxid. Redox. Signal. **9**, 1211 (2007)
55. J. Tatum, R.J. Kelloff, R.J. Gillies et al., Int. J. Radiat. Biol. **82**, 699 (2006)
56. M. Höckel, K. Schlenger, C. Knoop, P. Vaupel, Cancer Res. **51**, 6098 (1991)
57. P. Vaupel, A. Mayer, M. Höckel, Eur. J. Gynaecol. Oncol. **27**, 142 (2006)
58. M. Höckel, K. Schlenger, S. Höckel, B. Aral, U. Schäffer, P. Vaupel, Int. J. Cancer **79**, 365 (1998)
59. P. Vaupel, O. Thews, A. Mayer, S. Höckel, M. Höckel, Strahlenther. Onkol. **178**, 727 (2002)
60. M. Höckel, C. Knoop, K. Schlenger et al., Radiother. Oncol. **26**, 45 (1993)
61. M. Höckel, K. Schlenger, A. Aral, M. Mitze, U. Schäffer, P. Vaupel, Cancer Res. **56**, 4509 (1996)
62. G.L. Wang, G.L. Semenza, Proc. Natl. Acad. Sci. USA **90**, 4304 (1993)
63. G.L. Semenza, Crit. Rev. Biochem. Mol. Biol. **35**, 71 (2000)
64. G.L. Semenza, Trends Mol. Med. **8**(Suppl. 4), S62 (2002)
65. G.L. Semenza, Intern. Med. **41**, 79 (2002)
66. T.I. Goonewardene, H.M. Sowter, A.L. Harris, Microscop. Res. Techn. **59**, 41 (2002)
67. W.J. Whalen, J. Savoca, P. Nair, Amer. J. Physiol. **225**, 986 (1973)
68. H.A. Acker, D.W. Lübbers, M.J. Purves, Pflügers Arch. **329**, 136 (1971)
69. S. Barnett, E. Mulligan, L.C. Wagerle, S. Lahiri, J. Appl. Physiol. **65**, 2484 (1985)
70. M. Nordsmark, S.M. Bentzen, V. Rudat et al., Radiother. Oncol. **77**, 18 (2005)
71. P. Vaupel, Adv. Exp. Med. Biol. **645**, 241 (2009)
72. P. Vaupel, Adv. Exp. Med. Biol. **428**, 89 (1997)
73. P. Vaupel, M. Höckel, A. Mayer, Adv. Exp. Med. Biol. **701**, 101 (2011)
74. P. Vaupel, D.K. Kelleher, Adv. Exp. Med. Biol. **765**, 299 (2013)
75. H.J. Feldmann, M. Molls, T. Auberger, G. Stüben. In: Tumor oxygenation (Eds. P. Vaupel, D.K. Kelleher, M. Günderoth). Fischer: Stuttgart, Jena, New York, p. 31 (1995). ISBN 3–437–30784–3
76. P. Vaupel, S. Briest, M. Höckel, Wien. Med. Wschr. **152**, 334 (2002)
77. P. Vaupel, A. Mayer, S. Briest, M. Höckel, Cancer Res. **63**, 7634 (2003)
78. P. Vaupel, A. Mayer, Effects of anaemia and hypoxia on tumor biology, in *Anaemia in cancer, 2nd edit*. ed. by C. Bokemeyer, H. Ludwig (Elsevier, Edinburgh, 2005), p. 47
79. S. Runkel, E. Kaven, A. Wischnik, F. Melchert. In: Tumor oxygenation (Eds. P. Vaupel, D.K. Kelleher, M. Günderoth). Fischer: Stuttgart, Jena, New York, p. 233 (1995) ISBN 3–437–30784–3
80. J.E. Stone, R. Parker, G.B. Gilles, Eur. J. Gynaecol. Oncol. **26**, 31 (2005)
81. F. Kallinowski, H.J. Buhr. In: Tumor oxygenation (Eds. P. Vaupel, D.K. Kelleher, M. Günderoth). Fischer: Stuttgart, Jena, New York, p. 291 (1995) ISBN 3–437–30784–3
82. F. Kallinowski, H.J. Buhr. In: Tumor oxygenation (Eds. P. Vaupel, D.K. Kelleher, M. Günderoth). Fischer: Stuttgart, Jena, New York, p. 205 (1995) ISBN 3–437–30784–3
83. J. Mattern, F. Kallinowski, C. Herfarth, M. Volm, Int. J. Cancer **67**, 20 (1996)
84. S.J. Falk, R. Ward, N.M. Bleehan, Br. J. Cancer **66**, 919 (1992)
85. Q.T. Le, E. Chen, A. Salim et al., Clin. Cancer Res. **12**, 1507 (2006)
86. E. Lartigau, H. Randrianarivelo, M.F. Avril et al., Melanoma Res. **7**, 400 (1997)
87. M.E.B. Powell, D.R. Collinridge, M.I. Saunders et al., Radiother. Oncol. **50**, 167 (1999)
88. A.C. Kong, V.K. Mehta, Q.T. Le et al., Int. J. Radiat Oncol. Biol. Phys. **48**, 919 (2000)
89. S. Graffman, P. Björk, P. Ederoth, H. Ihse, Acta Oncol. **40**, 105 (2001)
90. R. Rampling, G. Cruikshank, A.D. Lewis et al., Int. J. Radiat. Oncol. Biol. Phys. **29**, 427 (1994)
91. N. Lawrentschuk, A.M.T. Poon, S.S. Foo et al., BJU Int. **96**, 540 (2005)
92. A. Carreau, B. El Hafny-Rahbi, A. Matejuk et al., J. Cell. Mol. Med. **15**, 1239 (2011)
93. E. Ortiz-Prado, J.F. Dunn, J. Vasconez et al., Am. J. Blood Res. **9**, 1 (2019)
94. T.P. Keeley, G.E. Mann, Physiol. Rev. **99**, 161 (2019)
95. V. Pietrobon, F.M. Marincola, J. Translat. Med. **19**, 1 (2021). https://doi.org/10.1186/s12967-020-02667-4
96. H. Acker, D.W. Lübbers, M.J. Purves, Pflügers Arch. **329**, 136 (1971)

97. W.J. Whalen, J. Savaca, P. Nair, Am. J. Physiol. **225**, 986 (1973). https://doi.org/10.1152/ajplegacy.1973.225.4.986
98. H. Landgraf, A.M. Ehrly, Aktuelle Geront. **10**, 511 (1980)
99. S.M. Santilli, V.D. Fiegel, D.R. Knighton, Hypertension **19**, 33 (1992)
100. M.M. Winburg, B.B. Howe, H.R. Weiss, J. Pharmacol. Exp. Ther. **176**, 184 (1971)
101. A.J. Moss, Cardiovasc. Res. **3**, 314 (1968)
102. L. Wiener, W.P. Santamore, A. Venkataswarmy et al., Clin Cardiol. **5**, 431 (1982)
103. P. Vaupel, Committee for European Education in Anaesthesiology (CEEA), Lecture Course No.4, Odessa, Ukraine (2019)
104. D.K. Harrison, P. Vaupel, Adv. Exp. Med. Biol. **812**, 25 (2014)
105. W. Wang, C. Winlove, C.C. Michel, J. Physiol. **549**, 855 (2003)
106. N.T.S. Evans, P.F.D. Naylor, Respir. Physiol. **2**, 46 (1966)
107. M. Hartel, P. Illing, J.B. Mercier, J. Lademann, G.D. Daeschlein, G. Hoffmann, G.M.S. Krankenhyg, Interdiscip. **2**, doc53 (2007)
108. Lempesis, R.L.J. van Meijel, K.N. Manolopoulos, G.H. Gossens, Acta Physiol. (Oxf.) **228**, e13298 (2020). https://doi.org/10.1111/apha.13298
109. M. Pasarica, O.R. Serada, L.M. Redmande, Diabetes **58**, 718 (2009)
110. H.M. Lawler, C.M. Underkofler, P.A. Kern et al., J. Clin. Endocrinol. Metab. **101**, 1422 (2016)
111. G.H. Gossens, M. Vogel, R.G. Vink et al., Diabetes Obes. Metabol. **20**, 2286 (2018)
112. L. Hodson, Adipocyte **3**, 75 (2014)
113. H. Günther, G. Aumüller, S. Kunke, P. Vaupel, G. Thews, Res. Exp. Med. **163**, 251 (1974)
114. H.J. Schurek, U. Jost, H. Baumgärtl et al., Am. J. Physiol. Renal Physiol **259**, F910 (1990)
115. J.L. Zhang, G. Morell, H. Rusinek et al., Am. J. Physiol. Renal Physiol. **306**, F597 (2014)
116. A. Dyson, F. Simon, A. Seifritz et al., Intensive Care Med. **38**, 1868 (2012)
117. P.O. Carlsson, F. Palm, A. Andersson, P. Liss, Diabetes **50**, 489 (2001)
118. C.A. Jacobi, H.V. Zieren, J.M. Müller, F. Adili, H. Pichlmaier, Eur. Surg. Res. **28**, 26 (1996)
119. P.O. Carlsson, P. Liss, A. Andersson, L. Jansson, Diabetes **47**, 1027 (1998)
120. P.J. Kinnala, K.T. Kuttila, J.M. Grönroos et al., Scand. J. Gastroenterol. **37**, 845 (2002)
121. T. Kietzmann, Redox Biol. **11**, 622 (2017)
122. P. Vaupel, P. Wendling, H. Thome, J. Fischer, Klin. Wschr. **55**, 239 (1977)
123. A. Mayer, M. Höckel, A. Wree, C. Leo, L.-C. Horn, P. Vaupel, Cancer Res. **68**, 4719 (2008)
124. J.A. Spencer, F. Ferraro, E. Roussakis et al., Nature **508**, 269 (2014)
125. F. Jung, H. Kessler, G. Pindur et al., Hemorheol. Microcirc. **21**, 25 (1999)
126. H. Landgraf, D. Schulte-Huermann, C. Vallbracht, A.M. Ehrly, Presse Med. **23**, 164 (1994)
127. P. Vaupel, J. Neuro-Oncol. **22**, 261 (1994)
128. J. Dings, J. Meixensberger, A. Jäger et al., Neurosurgery **43**, 1082 (1982)
129. I.M.H. van Buggenum, G.L. van Heijde et al., Br. J. Ophthalm. **80**, 567 (1996)
130. R.A. Linsenmeier, H.F. Zhang, Progr. Retinal Eye Res. **58**, 115 (2017)
131. M. Kwan, J. Niinikoski, T.K. Hunt, Invest. Ophthalmol. **11**, 108 (1972)
132. P.W. Davies, F. Brink Jr., Rev. Sci. Instrum. **13**, 542 (1942). https://doi.org/10.1063/1.1769961
133. D.B. Cater, I.A. Silver, Br. J. Radiol. **31**, 340 (1958)
134. P. Vaupel, K. Kallinowski, S. Dave, H. Gabbert, G. Bastert, Adv. Exp. Med. Biol. **191**, 737 (1985)

Authors and Affiliations

Peter Vaupel[1,2,3] · Ann Barry Flood[4] · Harold M. Swartz[4,5,6]

[1] Department of Radiation Oncology, University Medical Center, University of Freiburg/Brsg., Freiburg im Breisgau, Germany

[2] German Cancer Research Center (DKFZ), German Cancer Consortium (DKTK), Partner Site Freiburg, Heidelberg, Germany

[3] Department of Radiation Oncology, University Medical Center, University of Mainz, Langenbeckstrasse 1, 55131 Mainz, Germany

[4] Department of Radiology, Dartmouth Medical School, Hanover, NH, USA

[5] Department of Medicine, Section of Radiation Oncology, Dartmouth-Hitchcock Medical Center, Lebanon, NH, USA

[6] Thayer School of Engineering, Dartmouth College, Hanover, NH, USA